PAUL SCHERRER INSTITUT

Memorandum

Date: September 11, 2000

From: Thomas Prokscha
Phone: 42 75
Room: WLGA/B15
E-mail: Thomas.Prokscha@psi.ch

To: LEM group
cc:

Run12, thickness dependence of moderation efficiency

The analysis of the measured thickness dependence of the moderation efficiency ϵ_{mod} for s-N_2 and s-Ar on patterned Ag substrate is summarized. I used the offline calibration data by Rustem, see Tab. 1., to determine the layer thicknesses obtained during Run12 measurements. The comparison between measured and estimated (for sticking coefficient = 1) deposition rates shows that the local pressure at the moderator is about ten times larger than the measured pressure at the Penning gauge. The experimental rate dependence on pressure is nearly linear, but increasing the pressure by 10 yields a smaller rate increase by 6 - 8.

Table 1: Deposition rates measured by Rustem (22.11.-2.12.99, UHV LB3, p.175) on a micro balance mounted at the moderator position. The deposition pressure is the measured pressure at the Penning gauge outside the cryostat shields. The deposition procedure was repeated for some pressures. In this case, I took the mean value. The rates are reproducible within 10% which gives the relative error in the thickness determination. The estimated rate is taken from Elvezio's calculation, LB33, p.73.

Gas	deposition pressure [mbar]	measured rate [nm/s]	estimated rate [nm/s]
N_2	1×10^{-7}	0.11	0.009
	3×10^{-7}	0.24	0.028
	1×10^{-6}	0.73	0.092
	3×10^{-6}	1.49	0.277
	6×10^{-6}	2.87	0.554
	1×10^{-5}	4.94	0.923
Ar	1×10^{-7}	0.06	0.006
	3×10^{-7}	0.16	0.019
	1×10^{-6}	0.41	0.064
	3×10^{-6}	1.04	0.194
	6×10^{-6}	1.88	0.386
	1×10^{-5}	3.38	0.644
Kr	1×10^{-7}	0.04	0.004
	1×10^{-6}	0.25	0.036
	1×10^{-5}	1.89	0.360

The dependence of the moderation efficiency on the layer thickness d is shown in Figs. 1 and 2, where I used the online efficiencies, LB33 p.40-75, which were determined for same peak interval for s-N_2 and s-Ar. No computer busy correction was applied, which in all cases amounts to less than 1%.

The aim of the s-N_2 measurement was to test, if we can directly measure the gain in ϵ_{mod} due to the surface structure. The idea is, that, if increasing the layer thickness to more than a few μm, the s-N_2 possibly starts to fill the V-grooves rather than to continue growing parallel to the surface. In this case, one should have essentially a flat moderator when increasing the thickness to more than 20 μm, which is the depth of the V-grooves. However, we didn't observe this effect, thus implying that filling of the structure does not occur up to layer thicknesses of order 30 μm. The step of $\sim 30\%$ in ϵ_{mod} in the center part of Fig. 1 can not be attributed to a filling of the grooves, since it appears already at a thickness $d = 500$ nm. The step is probably caused due to a - what ever - change in the moderator, since the step was obtained after changing the deposition pressure from 1×10^{-7} mbar to 3×10^{-6} mbar. Also, the open square data point (deposition at 3×10^{-6} mbar for 600 s on clean substrate, our former "standard" layer) in the center part of Fig. 1 lies about 20% above the closed circle points. This additionally implies, that something's wrong, because a 20 s deposition at 3×10^{-6} mbar yields the same result than a corresponding longer evaporation time at 1×10^{-7} mbar, see bottom part of Fig. 1.

The slow decrease of ϵ_{mod} for increasing layer thicknesses above 1 μm can be attributed to the decreasing stop density near the moderator surface, see Fig. 3. Experimentally, we observe a decrease of ϵ_{mod} of about 20% when adding 30 μm of s-N_2, whereas the simulation predicts a larger decrease of 30%.

The s-Ar thickness dependence could only be measured up to about 500 nm due to unstable HV at the moderator at larger thicknesses. There appears to be an anomaly between 20 nm and 35 nm, see Fig. 2 bottom, where the slope of $\epsilon_{mod}(d)$ increases. However, the reproducibility of this shape ought to be checked. Maybe, it's just due to experimental uncertainties in preparing such thin layers: the first data points were taken with a very short deposition time of 10 s.

The comparison of s-N_2 and s-Ar data is shown in Fig. 4 for $d < 180$ nm. There are the following differences:

1. The saturation of $\epsilon_{mod}(d)$ for s-N_2 is at $d \sim 60$ nm. For s-Ar, it is about twice, $d \sim 120$ nm. Therefore, the escape depth for s-Ar is larger than for s-N_2 (there will be some fitting later...).
2. The slope of $\epsilon_{mod}(d)$ is larger for s-N_2 than for s-Ar. This implies a higher escape probability for an epithermal muon moving in s-N_2. This follows, if a one-dimensional diffusion model is a valid description for the escape of epithermal muons from the layer, which will be discussed below.
3. There are about two times more slow muons generated in s-N_2 after deposition of the first few nm.

Elvezio derived the solution for a one-dimensional diffusion model (see his St. Andrews report in *Muon Science*) for the stationary flux of epithermal muons. In terms of the moderation efficiency it

can be written as[1]

$$\epsilon_{mod}(d) = N_{stop} \cdot P_{esc} \cdot L \cdot \tanh\,(\frac{d}{2L}), \tag{1}$$

with N_{stop} the number of muons stopped per nm, P_{esc} the escape probability for a muon, and L the escape depth. The escape probability is determined by the fraction of muons, which do not have formed muonium (Mu), and by the fraction of muons, which do have the possibility to reach the surface. For an isotropic distribution of muons inside the layer, this amounts to 50% at the most. The positive work function of muons in the solid gas layer also reduces the escape probability. However, since the work function is of order eV it mainly affects only the low energy tail of the energy spectrum, and additionally, it ought to be similar in s-N_2 and s-Ar. Therefore, I will neglect it in the following discussion.

Before doing any fits, we can look to some implications of Eq. 1. For small arguments of $\tanh\,(x)$ ($x < 1$, that is $d < L$ in our case), we have $\tanh\,(x) \sim x$. In this case, L cancels in Eq. 1 and the slope is determined by the pre-factor $N_{stop} \cdot P_{esc}$. This means, that for s-N_2 the pre-factor must be larger than for s-Ar. However, the stop density N_{stop} in s-N_2 is smaller by about 15% (valid for our experimental conditions, see my memo *Moderation efficiency of flat and patterned moderator*, May 24, 2000) due to its lower density. Therefore, a smaller epithermal (or prompt) muonium fraction, yielding a larger P_{esc}, is needed in s-N_2 to compensate for the smaller stop density. However, this would be in contradiction to Mu fractions f_{Mu} measured in gases, where at 1 bar pressure f_{Mu}(N_2) $\sim$ 84%, and f_{Mu}(Ar) $\sim$ 74% [Fleming et al., Phys.Rev.A26, 2527 (1982)]. These are attributed to prompt fractions, that means, Mu was formed at epithermal energies and thermalized as Mu. From data by Storchak et al., Phys.Rev.B59, 10559 (1999), the prompt Mu fraction in s-N_2 can be estimated to range between 40% and 65% [2], which is in contradiction to the gas data. However, they did not make any comparison to the gas data. Their s-Ar data are not yet published. From Storchak's talk at the 1. LEM workshop [PSI, 1999] a prompt Mu fraction $< 70\%$ can be estimated in s-Ar. Our LE-μSR Run12 data of Mu in s-Ar and s-N_2 yield preliminary Mu fractions of about 60% and 50%, respectively. So, this is already the right direction, but we measured only the *thermal* fraction, which should be distinct from the prompt fraction, because the thermal fraction includes delayed Mu formation via convergence of a muon and a spur electron. But maybe, we do not have a big difference between prompt and thermal fraction (as in the bulk measurements), because, due to the low energy of implanted muons, the number of track electrons is two orders of magnitude smaller. This might reduce the Mu formation via convergence with an electron, but this still must be proven experimentally. Our data on the thickness dependence indicate a smaller prompt Mu fraction in s-N_2 than in s-Ar. So, Storchak's and our measurements qualitatively agree, and they show, that the prompt fractions in the solids differ from the gas data (or that the Mu fractions in 1 bar gas are not only determined by the prompt fractions).

[1] Although the solution is derived for a plane moderator it might be applicable also in the case of a patterned moderator, because we only have to consider the diffusion perpendicular to the surface. The extraction of the muons from the structure after exit through the surface is a separate step.

[2] I estimate a prompt Mu fraction of 40% from their measured B-field dependence of the Mu signal in β-N_2. Our moderator, which is formed at T < 35 K, is in the α phase. Using their E-field dependence of the Mu fraction in α-N_2, one can estimate a prompt Mu fraction of 65%. Since they did not explicitly derive the prompt fractions, they did not discuss it at all. Basically, the prompt epithermal fraction should not depend on the solid state phase.

To determine the escape depth L I started to fit Eq. 1 to the data, modified by an offset ϵ^0_{mod}:

$$\epsilon_{mod}(d) = N_{stop} \cdot P_{esc} \cdot L \cdot \tanh\left(\frac{d}{2L}\right) + \epsilon^0_{mod}, \tag{2}$$

where ϵ^0_{mod} is the measured efficiency for the blank substrate, which is of order $100/10^8$ $S1_{cl}$. However, the agreement between fit and data is not very well. This is mainly due to the very steep increase just after putting the first layer on the substrate. A more satisfactory fit is obtained by starting the fit at $d > 0$. The fit result is shown in Fig. 5. For s-N_2, the fit is already quite well with a $\chi^2_{red} = 1.5$, whereas for s-Ar, it is not as good ($\chi^2_{red} = 7.1$). The fitted offsets for s-Ar, $\epsilon^0_{mod} = 345(6)$, and for s-$N_2$, $\epsilon^0_{mod} = 720(16)$, do not agree with the measured offsets of 112(8) and 88(6), respectively. Shifting the s-N_2 data (for $d > 0$) by 8.6 nm to larger d's allows to obtain an agreement between measured and fitted offset with a $\chi^2_{red} = 1.3$ close to one. For s-Ar, such a procedure fails, whatever shift is used. From the calibration measurements there is no justification to introduce such a large shift, so, it appears to be an arbitrary correction in order to get a better fit when using all data points.

Assuming that the layer thicknesses are correct and that there is no additional effect due to the surface structure (to avoid this uncertainty a flat substrate should be used), what is the physical meaning of the very steep increase at $d = 0$ yielding the deviation between fitted and measured ϵ^0_{mod}? It could be the following: the beam leaving the substrate at energies below hundred eV should be mainly a Mu beam. For Al, which should give approximately the same charge fractions like Ag, a Mu fraction of 75% was measured at 1 keV, and this is expected to increase to about 90% at epithermal energies. Between 50 eV and 100 eV, the cross sections for electron loss and electron capture (scaled from proton data) in N_2 and Ar are of order 10^{-16} cm^2 (see Fig. 6), resulting in mean free paths for electron loss and capture of the order of nm. Therefore, a few-nm thin layer of s-N_2 or s-Ar could efficiently remove electrons from Mu, if the equilibrium Mu fraction in the gas layer is lower than that of the Ag substrate. We have seen in the discussion above, that the epithermal (prompt) Mu fraction in the solid gas layers probably amounts to about 50%, which is smaller than the $\sim 90\%$ of the beam coming out of the substrate. The electron loss cross section is about two times larger in N_2, which should translate into a higher offset than in Ar, in agreement with our data.

The equilibrium of charge states formed in the metal is destroyed by the moderator layer. In the solid gas layer it needs several mean free paths of charge changing collisions to build up a new charge state equilibrium. We may write down the following differential equation to solve the problem analytically:

$$\begin{aligned} \frac{\partial}{\partial d} f_{Mu}(d) &= -\frac{1}{\lambda_l} f_{Mu}(d) + \frac{1}{\lambda_c} f_{\mu}(d) \\ &= -\frac{1}{\lambda_l} f_{Mu}(d) + \frac{1}{\lambda_c} \left[1 - f_{Mu}(d)\right], \end{aligned} \tag{3}$$

with $f_{Mu}(d)$, $f_{\mu}(d)$ the Mu and μ^+ fractions at depth d and $[f_{Mu}(d) + f_{\mu}(d)] = 1$; $\lambda_l = 1/(n \cdot \sigma_l)$ the mean free path for electron loss of a Mu atom, n the number of atoms per cm^3, σ_l the electron loss cross section; $\lambda_c = 1/(n \cdot \sigma_c)$ the corresponding variables for electron capture of a muon. Equation 3 represents a simplification, because $\lambda_{l,c} = \lambda_{l,c}(d)$, are a function of d due to the energy dependence of the cross sections. After each collision the energy, and therefore the cross sections, changes. For simplicity, I will neglect this in the following.

The differential equation above is of the form

$$f' + a \cdot f = b, \tag{4}$$

with solution

$$f(d) = C \cdot \exp(-a \cdot d) + \frac{b}{a}, \tag{5}$$

where the constant C is determined by the boundary condition at $d = 0$. The Mu fraction in dependence on d is then

$$f_{Mu}(d) = \left(f_{Mu}(0) - \frac{\lambda_l}{\lambda_l + \lambda_c} \right) \cdot \exp\left[-(\frac{1}{\lambda_l} + \frac{1}{\lambda_c}) \cdot d \right] + \frac{\lambda_l}{\lambda_l + \lambda_c}, \tag{6}$$

where $f_{Mu}(0)$ is the Mu fraction of the beam exiting the Ag substrate. For $d \to \infty$ the Mu fraction becomes

$$\frac{\lambda_l}{\lambda_l + \lambda_c} = \frac{\sigma_c}{\sigma_l + \sigma_c}, \tag{7}$$

the well known steady state fraction.

In our measurement, we are interested in the muon fraction $f_\mu(d) = [1 - f_{Mu}(d)]$. We see, that this must follow a $[1 - \exp(d)]$ instead of $\tanh(d)$ in case of diffusion. The difference between $\tanh(d)$ and $[1 - \exp(d)]$ is, that saturation is reached "faster" in $\tanh(d)$ (the "bend" of the function is sharper).

So, let's go back to the data in Fig. 5. The s-Ar as well as the s-N_2 data appear to consist of two components: a very fast increase during the first few nm followed by a softer slope. However, the s-N_2 data are quite well fitted by the $\tanh(d)$ with offset, Eq. 2, after the step at $d = 0$. There is no hint for a $[1 - \exp(d)]$ behaviour. A possible explanation could be, that a new charge state equilibrium builds up too fast (within the first few nm) to be observed. For the s-Ar data the step extends over a range of about 10 nm including a few data points, and we can try to indentify this step by the Mu stripping process, Eq. 6. If this is correct, a two component fit consisting of Eq. 1 (epithermal μ^+ diffusion) and $f_\mu(d) = [1 - f_{Mu}(d)]$ from Eq. 6 (Mu stripping) should fit to the data:

$$\begin{aligned} \epsilon_{mod}(d) &= N_{stop} \cdot P_{esc} \cdot L \cdot \tanh(\frac{d}{2L}) + \\ &\quad N_{fast} \cdot \left\{ 1 - \left[\left(f_{Mu}(0) - \frac{\lambda_l}{\lambda_l + \lambda_c} \right) \cdot \exp\left(-(\frac{1}{\lambda_l} + \frac{1}{\lambda_c}) \cdot d \right) + \frac{\lambda_l}{\lambda_l + \lambda_c} \right] \right\} \\ &= N_{stop} \cdot P_{esc} \cdot L \cdot \tanh(\frac{d}{2L}) + N_{fast} \cdot f_\mu(d), \end{aligned} \tag{8}$$

where N_{fast} is the total number of muons (including muonium) coming out of the substrate which may contribute to the M3S1 TOF peak interval of interest, i.e. muons with energies below ~ 150 eV. Equation 8 is the same as Eq. 2, where ϵ^0_{mod} is substituted by $N_{fast} \cdot f_\mu(d)$. The fit of Eq. 8 to the s-Ar data is shown in Fig. 7a). The dashed curves indicate the two contributions, where $N_{fast} \cdot f_\mu(d)$ is a flat line for $d > 2$ nm. This part generates the steep increase at the very beginning and reaches

saturation at about $d = 2$ nm. A better fit is obtained when we allow the $f_\mu(d)$ contribution to decrease with increasing d:

$$\epsilon_{mod}(d) = N_{stop} \cdot P_{esc} \cdot L \cdot \tanh\left(\frac{d}{2L}\right) + N_{fast} \cdot f_\mu(d) \cdot \exp\left(-\frac{d}{l_d}\right), \tag{9}$$

where l_d is the characteristic length for the decrease of $f_\mu(d)$. The fit is shown in Fig. 7b). At the moment, I have no physical argument for the introduction of this decreasing fraction, so it appears to be an arbitrary choice to get the function better fit. Additionally, it is in contradiction to the procedure with the s-N_2 data, where a constant, non-decreasing offset fits very well to the data. Anyway, we can have a look on the fit parameters which seem to be reasonable in both cases. The muonium fraction of the beam when emerging from the Ag substrate is about 90% which is the expected fraction for energies of order 100 eV. The mean free paths for electron loss and electron capture in the s-Ar layer are of order 1 nm, as they should be. Using Eq. 7, we can estimate the steady state epithermal Mu fractions in s-Ar to 71% in Fig. 7a), and to 58% in Fig. 7b)[3]. The larger Mu fraction in Fig. 7a) causes a smaller "stop-escape" probability for epithermal muons, $N_{stop} \cdot P_{esc} = 74.7$ 1/nm, compared to $N_{stop} \cdot P_{esc} = 95.5$ 1/nm in Fig. 7b). The relative change is determined by the relative change of the Mu fractions, so, this looks ok, too. The escape depths are about 35 nm, which was the value obtained by fitting Eq. 2 to the data, see Fig. 5. Taking into account the "stop-escape" probability of s-N_2, $N_{stop} \cdot P_{esc} = 119.2$ 1/nm (Fig. 5), and the $\sim$ 15% reduced stop density in s-N_2, we can estimate the epithermal Mu fraction in s-N_2 to about 45% and 38%, respectively, when using the $N_{stop} \cdot P_{esc}$ data from Fig. 7a) and b):

$$\frac{N^{Ar}_{stop} \cdot P^{Ar}_{esc}}{N^{N_2}_{stop} \cdot P^{N_2}_{esc}} = \frac{N^{Ar}_{stop} \cdot (1 - f^{Ar}_{Mu})}{0.85 \cdot N^{Ar}_{stop} \cdot (1 - f^{N_2}_{Mu})} = \frac{(1 - f^{Ar}_{Mu})}{0.85 \cdot (1 - f^{N_2}_{Mu})}$$

This agrees with the Storchak data for β-s-N_2, and approximately with our preliminary result of Run12 ($\sim 50\%$ *thermal* Mu fraction in s-N_2). Although not everything fits into a consistent interpretation, we can conclude that the shape of $\epsilon_{mod}(d)$ at small d indicates that sizeable formation of epithermal μ^+ first starts with electron loss of Mu, followed by the real moderation process leading to a diffusion like dependence of $\epsilon_{mod}(d)$.

In the M3S1 TOF spectra a change in the width and peak position should be observable in dependence on d, although the Run12 TOF measurement is not very sensitive on changes in energy due to the relatively short path length between moderator and trigger detector, and the large acceleration of the epithermal μ^+ at the moderator. The blank substrate generates a flat energy spectrum of epithermal μ^+ [Thesis A. Hofer]. This results in a peak in the TOF spectrum due to i) the non-linear correspondence between time and energy spectrum, ii) the decreasing transmission of the transport system for increasing energy, and iii) the non one-to-one correspondence between time and energy bins (particles with different energy can be detected in the same time bin due to different path lengths in the transport system). When adding moderator layer to the blank substrate the energy spectrum starts to form a peak at $\sim$ 15 eV, thus shifting the position of the TOF peak to larger times and decreasing the width of the peak. I fitted the TOF spectra with a Lorentzian to obtain the peak position and half-width-at-half-maximum (HWHM). A Lorentzian fits better than a Gaussian because

[3] In Run12, we measured about 60% *thermal* Mu fraction in s-Ar.

the tails of TOF the peak, ranging up to $\sim$ 50 ns from the peak position, can not be represented by a Gaussian[4]. The mean peak position and the HWHM are shown in Figs. 8 and 9 for s-Ar and s-N_2, respectively. The shape of the thickness dependence is similar to that of $\epsilon_{mod}(d)$: a large slope at the beginning, followed by a region with decreasing slope approaching saturation at same thicknesses. The mean peak position shifts by about 1 ns to larger times, and the width is reduced by about 1 ns (without taking into account the experimental time resolution, which is about 1 ns). This variation can be attributed to the change of the energy distribution from a flat spectrum to a peaked spectrum with reduced width. The small difference between s-Ar and s-N_2 data at saturation – peak positions at TDC channel 522.8 and 523.0, and HWHM of 1.35 and 1.42 ns,respectively – can be attributed to the smaller width of the energy spectrum of epithermal μ^+ emitted from s-Ar [Thesis A. Hofer]. The continuos shift in peak position and the reduction of the width can be explained by the superposition of two distributions with different widths and peak positions: a broader distribution from the blank substrate (which can be represented by a Gaussian or a Lorentzian) or stripped Mu at the exit of the moderator layer, and a more narrow distribution due to the moderated μ^+. When fitting a single Lorentzian to the sum of both distributions, the peak position shifts and the width is reduced, if the contribution of the broad distribution keeps constant with d while the intensity of the other distribtion (moderated μ^+) is increasing. Saturation is reached when the number of moderated μ^+ no longer changes.

To summarize (and some addenda):

- The escape depth L_{Ar} of s-Ar is about 35 nm, which is 2.3 times larger than the escape depth of s-N_2, L_{N_2} =15 nm. The escape depths are determined by fitting Eq. 2 to the data, which is the solution of the diffusion model with a depth independent offset ϵ^0_{mod}.
- The larger slope of ϵ_{mod} in s-N_2 indicates a smaller prompt Mu fraction compared to s-Ar. For s-Ar, a prompt Mu fraction of 60-70% is estimated, from which a Mu fraction of about 40% is derived for s-N_2. These numbers do not agree with gas data at 1 bar, but they correspond to the fractions estimated from measurements in bulk solids [Storchak] as well as to our studies [Run12, *thermal* fraction].
- Although the escape depths between s-Ar and s-N_2 differ by a factor two the moderation efficiency of s-N_2 is only 20% lower. This can be mainly attributed to the larger offset ϵ^0_{mod} (Mu electron loss) and to less extent to the smaller prompt Mu fraction in s-N_2 (the active moderation volume is smaller, but it contains a larger number of epithermal μ^+). The greater contribution of stripped Mu to epithermal μ^+ emitted from s-N_2 could explain the larger width of the energy distribution.
- The step of $\epsilon_{mod}(d)$ at $d \sim 0$ indicates that Mu emerging from the Ag substrate efficiently loose the electron when adding a few nm of a moderator layer on the substrate. According to this interpretation, the generation of epithermal μ^+ is dominated by Mu stripping at small thicknesses, followed by the real moderation process at larger d's.
- The thicknesses are calibrated for a plane substrate. Taking into account the surface enlargement due to the V-groove structure, the thickness perpendicular to the groove walls ought to

[4]The simulation of the transport system shows, that the TOF distribution should be *Gaussian*! The long tails could be an indication for delayed epithermal μ^+ emission. This tail is absent in case of the blang Ag substrate.

be 1.7 times smaller. This would reduce the escape depths by the same factor. Using a plane substrate would avoid this uncertainty.

- The escape depth of s-Ar does not agree with earlier measurements, where we obtained 70 nm [St. Andrews article]. I tried some TRIM.SP simulation where only the elastic interaction was enabled: it shows that it is hard to reach more than 20 nm for L_{Ar}. So, the 70 nm might be too optimistic.
- If we will repeat these measurements, we should do it with S1M2 (longer path length) and low acceleration at the moderator in order to be more sensitive on the energy distribution.
- Other suggestions . . .

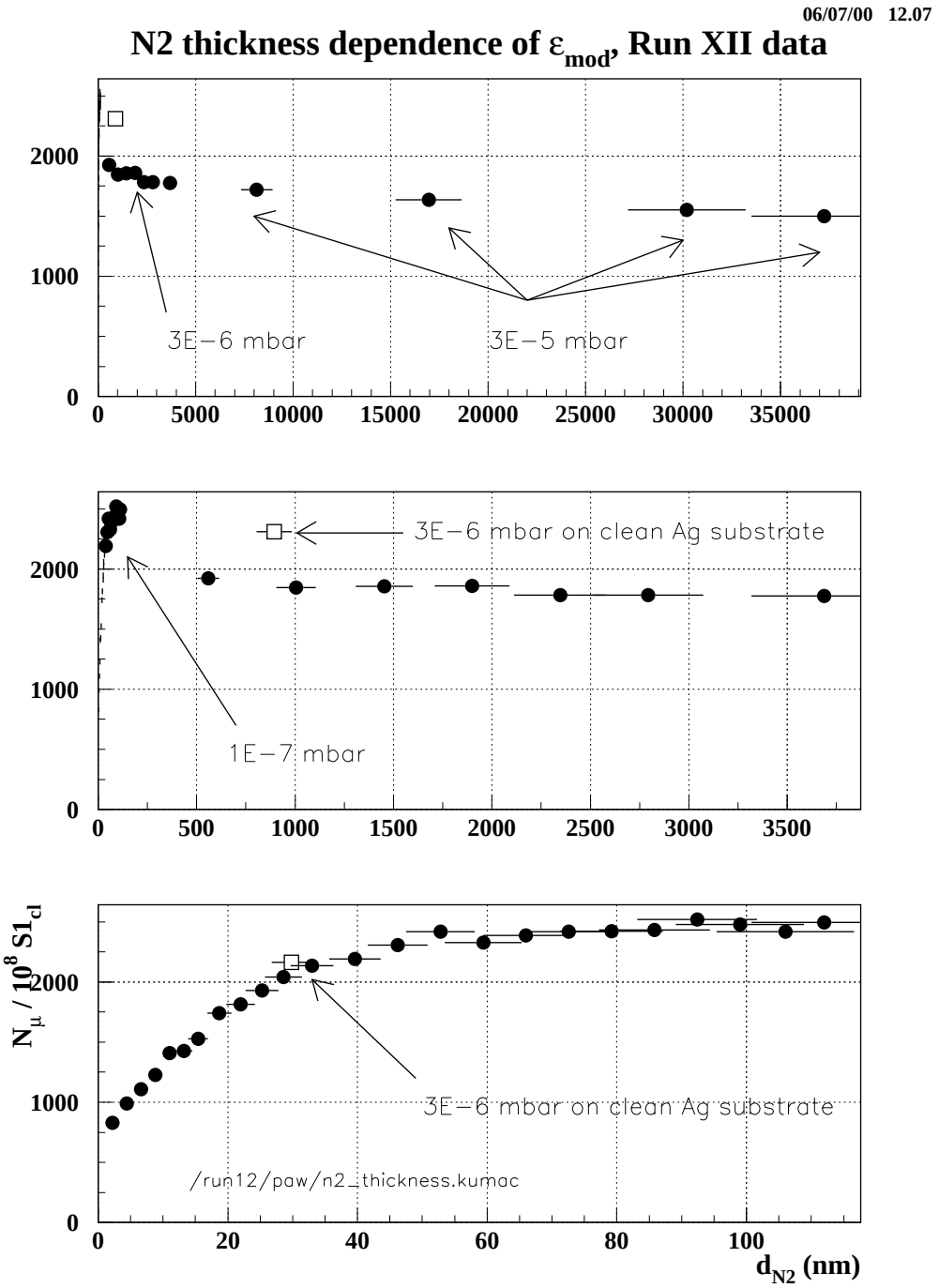

Figure 1: Dependence of moderation efficiency on s-N_2 layer thickness. Measurements were started with blank Ag substrate. Then, evaporation at 1×10^{-7} mbar was performed to add new s-N_2 on existing layer (bottom). The deposition pressure was increased to 3×10^{-6} mbar (center), and finally to 3×10^{-5} mbar (top). Open squares: deposition starting with blank Ag substrate. TOF M3S1 data, 7.5 kV settings. The horizontal error bars are determined by the 10% uncertainty of the thickness calibration.

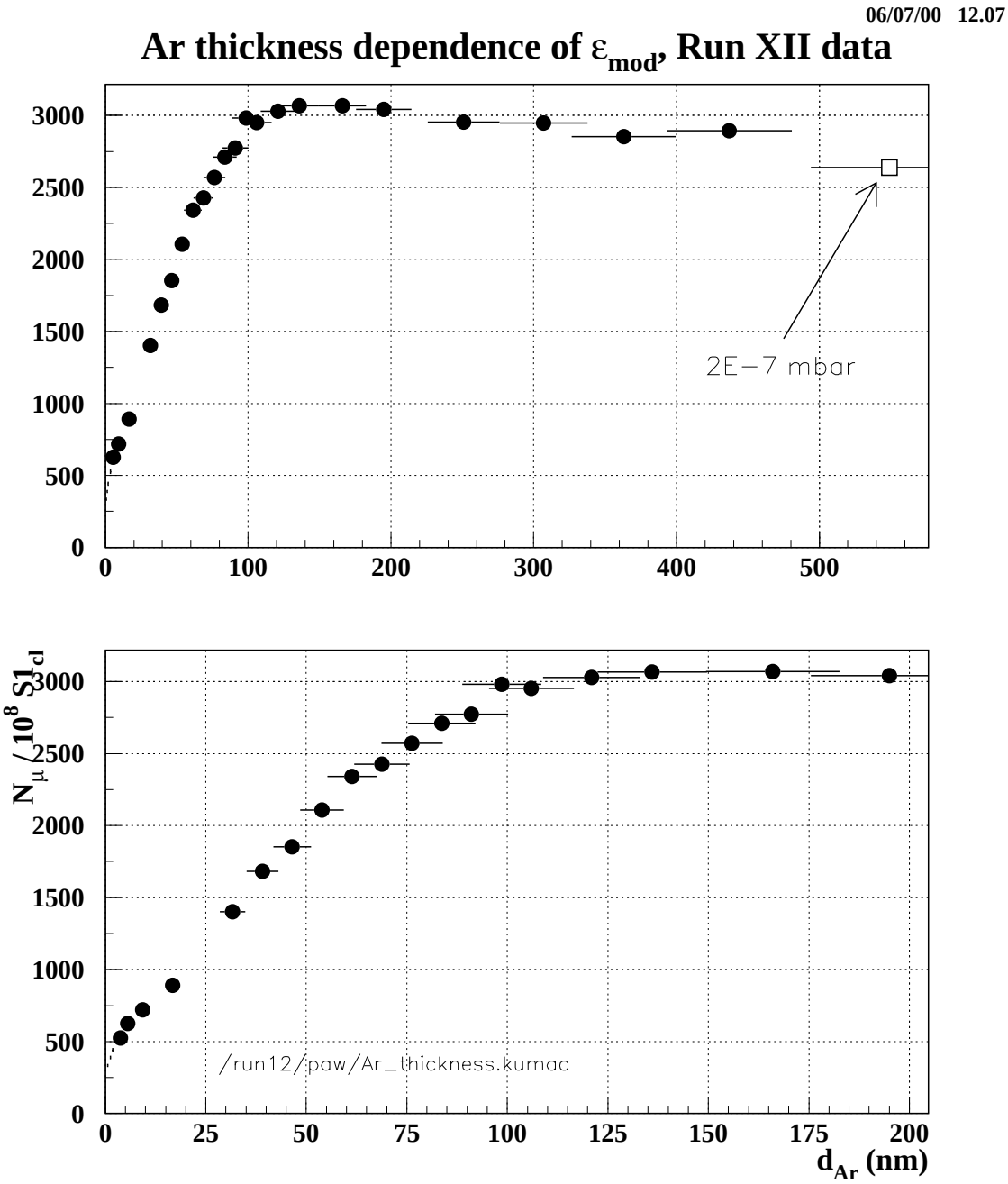

Figure 2: Dependence of moderation efficiency on s-Ar layer thickness. All measurements were performed at 1×10^{-7} mbar, except the last point (open square, $p = 2 \times 10^{-7}$ mbar). As in Fig. 1, measurements were started with blank Ag substrate, and new s-Ar was added on top of existing layer. TOF M3S1 data, 7.5 kV settings.

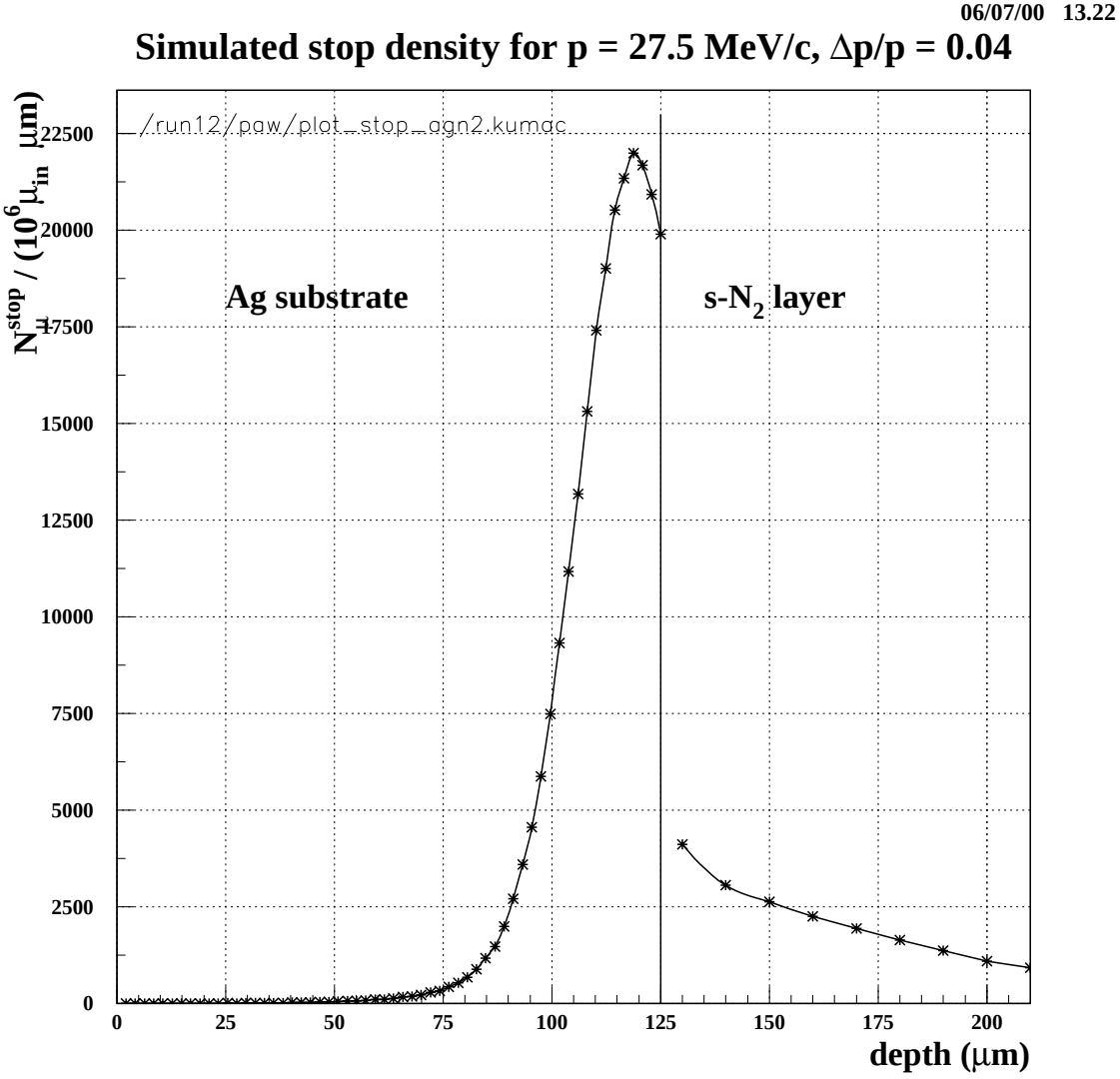

Figure 3: Simulated muon stop density in a 125-μm Ag substrate covered by a 100-μm s-N_2 layer, program MCV3K.

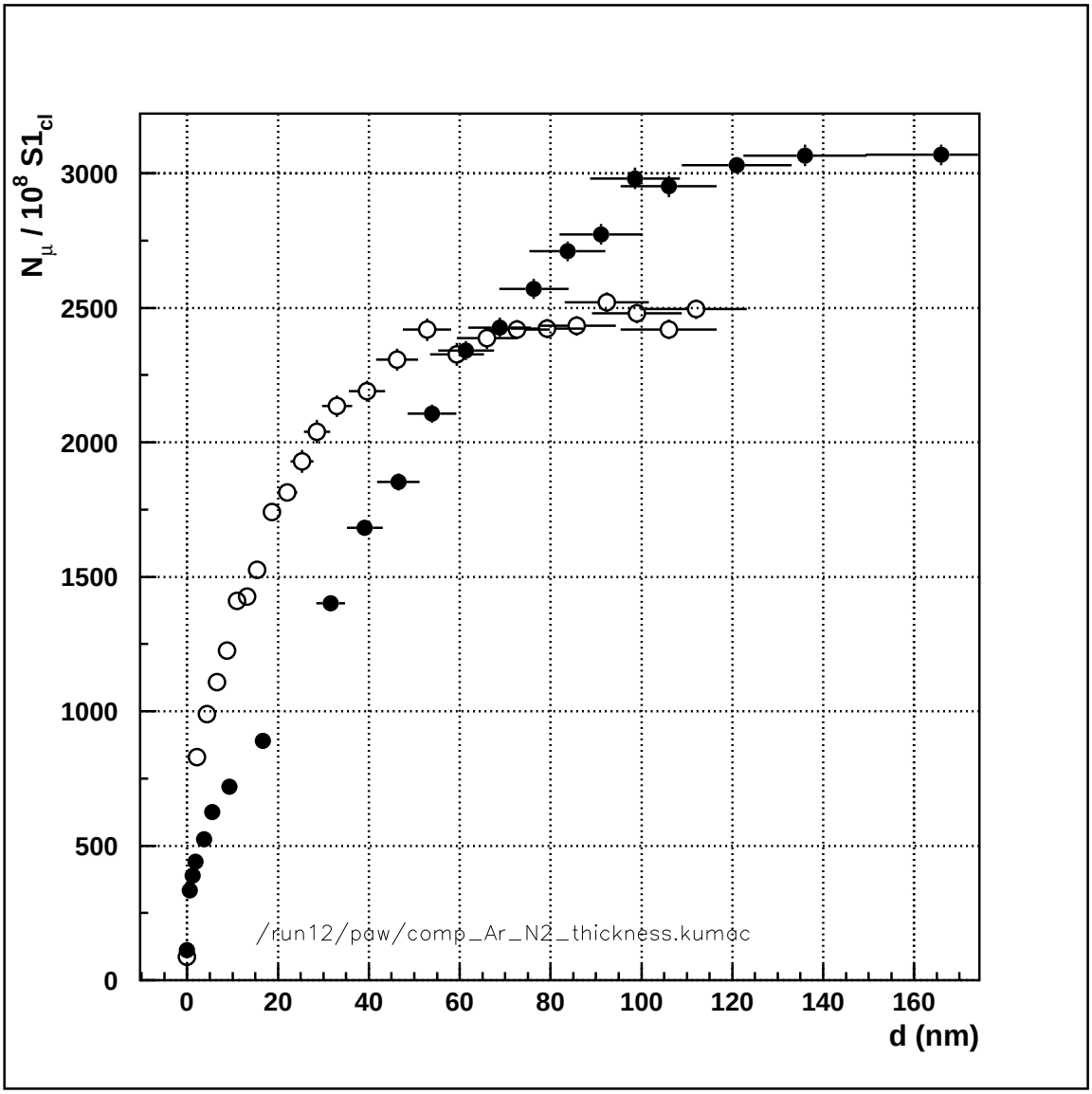

Figure 4: Comparison of $\epsilon_{mod}(d)$ for s-N_2 (open circles) and s-Ar (full circles).

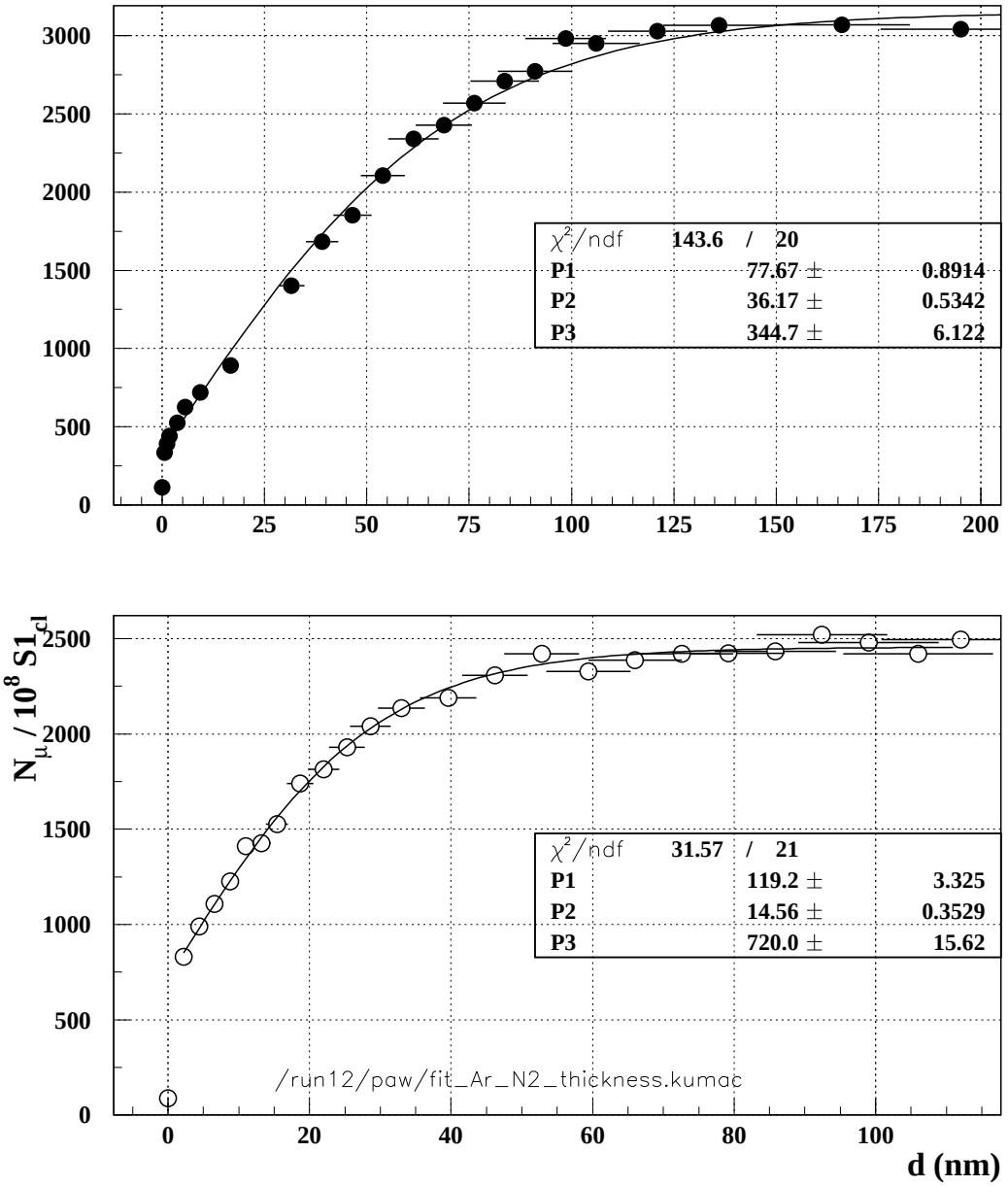

Figure 5: Fit of Eq. 2 to s-Ar (full circles) and s-N_2 (open circles) data. P1 $\equiv N_{stop} \cdot P_{esc}$ [1/nm], P2 $\equiv L$ [nm], and P3 $\equiv \epsilon^0_{mod}$. The measured offset for d = 0 nm is 112(8) in s-Ar, and 88(6) in s-N_2. These offsets do not agree with the fit result, which is discussed in the text.

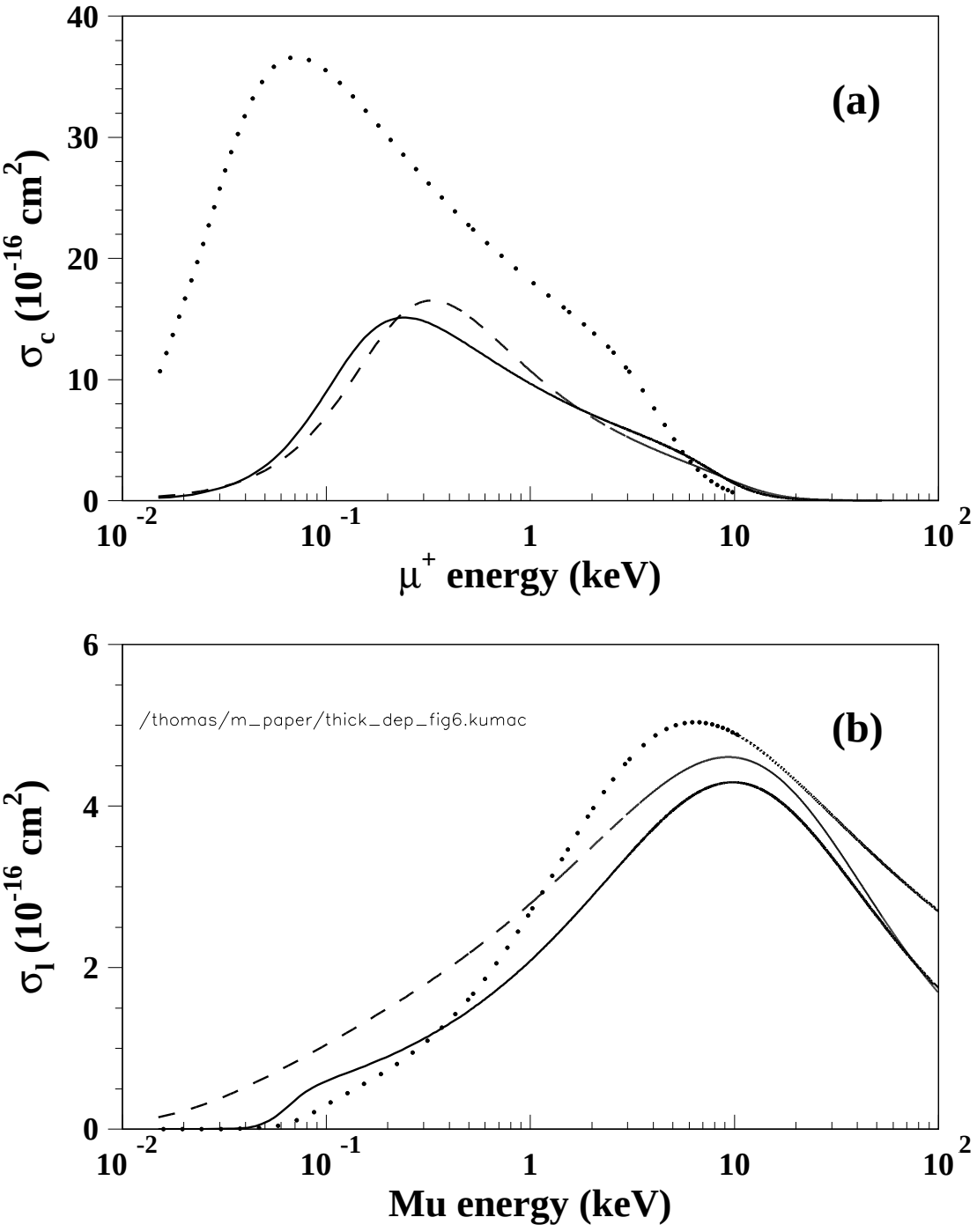

Figure 6: Velocity scaled cross sections of protons for (a) electron capture $\sigma_c(E)$ of μ^+, and (b) for electron loss $\sigma_l(E)$ of the Mu atom. Solid line, Ar; dashed line, N_2; dotted line, Xe, for comparison.

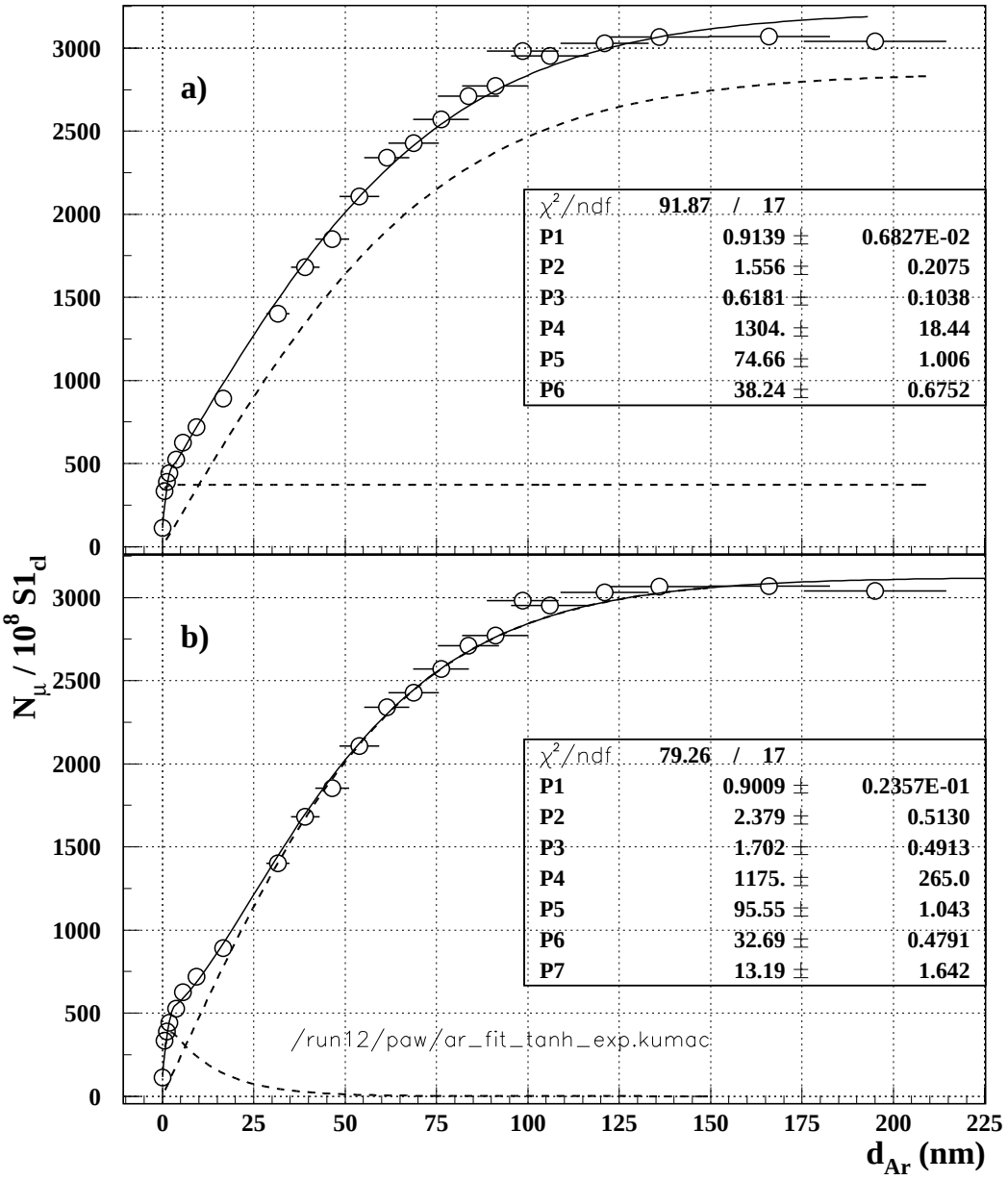

Figure 7: a) Fit of Eq. 8 to s-Ar data: P1= $f_{Mu}(0)$, the Mu fraction of the beam at the exit of the Ag substrate; P2= λ_l [nm], the mean free path for electron loss of Mu in s-Ar; P3= λ_c [nm], the mean free path for electron capture of μ^+ in s-Ar; P4= N_{fast}, the number of μ^+ and Mu with energies below 150 eV coming out of the Ag substrate; P5= $N_{stop} \cdot P_{esc}$ [1/nm], the number of stopped μ^+ times escape probability (in s-Ar); and P6= L [nm], the escape depth. b) Fit of Eq. 9 to the s-Ar data. All parameters as in a). P7= l_d [nm], the characteristic length for the decreasing contribution of $f_\mu(d)$ to ϵ_{mod}.

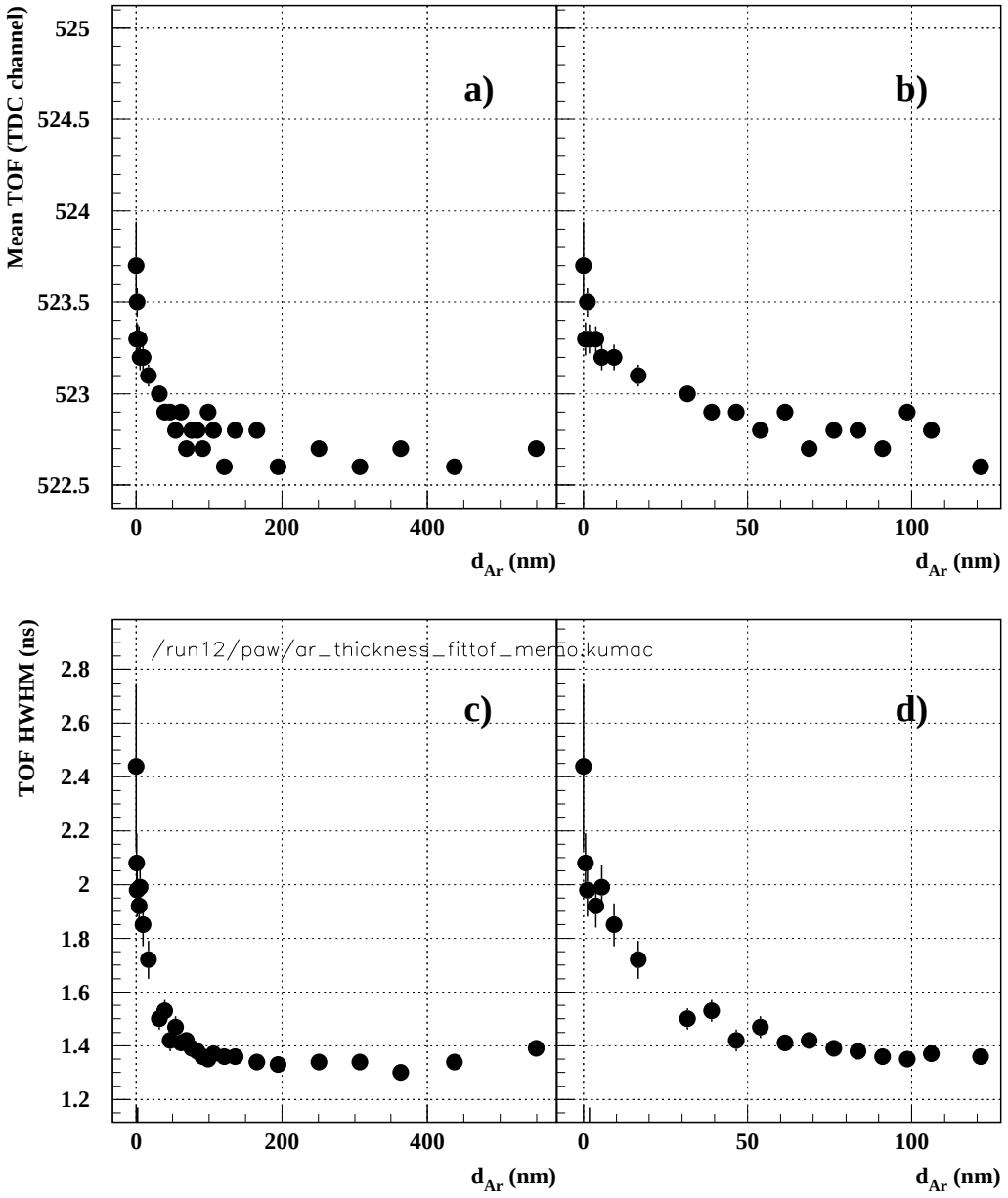

Figure 8: s-Ar: fit of a Lorentzian to the M3S1 time-of-flight (TOF) spectra to obtain the mean peak position,a) and b), and the HWHM, c) and d), as a function of moderator thickness d, 7.5 kV settings. One TDC channel corresponds to 1 ns. The TOF spectra were measured with reverse timing, that is decreasing TDC channel number means increasing TOF.

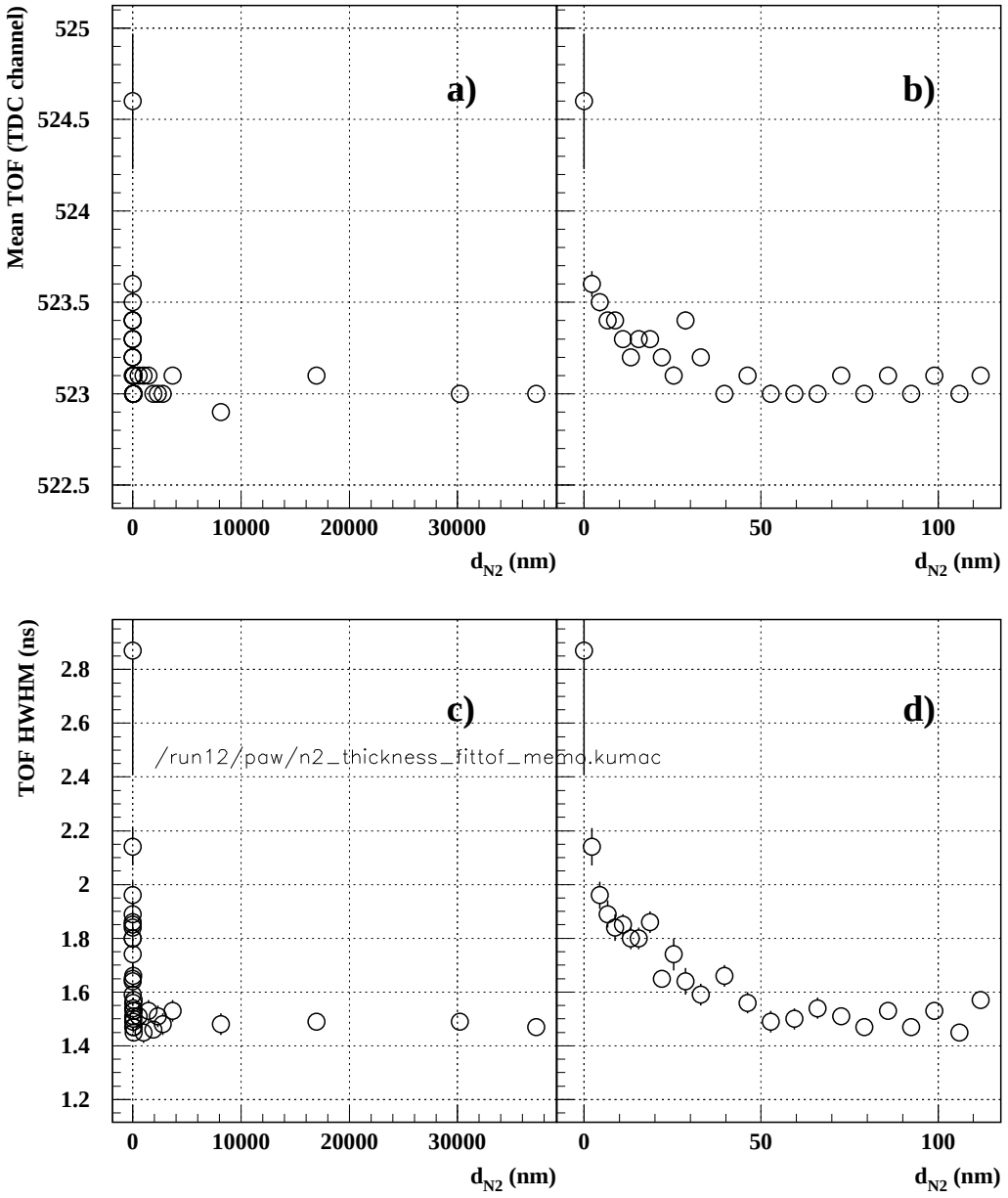

Figure 9: s-N_2: fit of a Lorentzian to the M3S1 time-of-flight (TOF) spectra to obtain the mean peak position,a) and b), and the HWHM, c) and d), as a function of moderator thickness d, 7.5 kV settings. One TDC channel corresponds to 1 ns. The TOF spectra were measured with reverse timing, that is decreasing TDC channel number means increasing TOF.